MODIFICATION OF HOMESTEAD HOLLOW AT THE INSIGHT LANDING SITE BASED ON THE DISTRIBUTION AND PROPERTIES OF LOCAL DEPOSITS. J. A. Grant[1], N. H. Warner[2], C. M. Weitz[3], M. P. Golombek[4], S. A. Wilson[1], E. Hauber[5], V. Ansan[6], C. Charalambous[7], N. Williams[4], F. Calef[4], T. Pike[7], A. DeMott[2], M. Kopp[2], H. Lethcoe-Wilson[4], and M. Banks, [1]Center for Earth and Planetary Studies, National Air and Space Museum, Smithsonian Institution, 6th at Independence SW, Washington, DC, 20560 (grantj@si.edu), [2]SUNY Geneseo, Dept. Geol. Sci., 1 College Circle, Geneseo, NY 14454, [3]Planetary Science Institute, 1700 East Fort Lowell, Tucson, AZ, 85719, [4]Jet Propulsion Laboratory, California Institute of Technology, Pasadena, CA, [5]German Aerospace Center (DLR), Inst. Planetary Research, [6]University of Nantes, Laboratory of Planetary and Geodynamics, [7]Imperial College, London, Department of Electrical and Electronic Engineering, [8]NASA Goddard Space Flight Center, Greenbelt, MD.

Introduction: The Interior Exploration using Seismic Investigations, Geodesy, and Heat Transport (InSight) mission landed at 4.50° N, 135.62° E [1] in what is likely a highly degraded ~20 m-diameter impact crater in Elysium Planitia dubbed "Homestead hollow" [2-5]. A HiRISE DEM confirms the hollow is up to ~0.8 m deep [3, 6]. Measurements from the DEM and lander images from the Instrument Deployment Camera (IDC) show the interior surface is quite flat down to the cm-scale and slopes <3° to the SE. The hollow lacks a significant elevated rim, but does show an abrupt increase in cobble to boulder size rocks around the margin relative to the interior. If the hollow is a degraded impact, its initial depth was ~3.5-4.0 m and it likely was bounded by a ~1 m high rim [3, 7] and fairly steep walls.

Homestead hollow probably formed ~500 million years ago [9, 10] into regolith derived from an underlying Hesperian-aged basaltic plain [9-12] and is one of many small craters in the area [2]: ~10 craters <10 m-diameter are in or near the hollow.

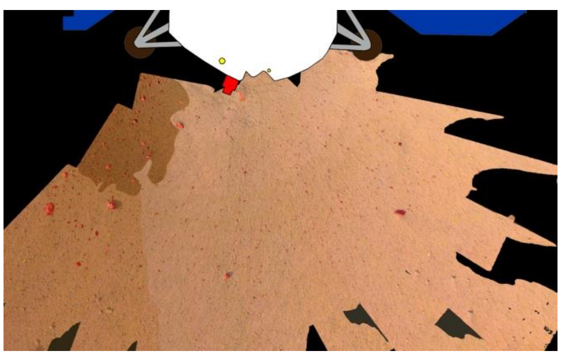

Figure 1. InSight WebGIS [13] composite of lander workspace and vicinity. IDC mosaic F2MMWKSSM1 (2 mm pixel-scale) overlain by Geology Group map of soils and rocks (red). Medium and dark brown indicate medium coarse sand to cobble unit and coarser sand to pebble unit, respectively. Light brown unit is finer sand to cobble unit. Rock density is higher in darker brown units. Lander footpad centers ~1.4 m apart. North is up.

Description: Mapping using lander images (Fig. 1) shows mostly sand to pebble-sized fines occur across the hollow floor [14] that is variably punctuated by mostly gravel/pebbles and cobbles. Many fragments closer to the lander, especially near the western front footpad, are reddish-brown, often appear platy and/or sometimes broken in place, and contrast with darker-gray, sub-angular pebbles observed elsewhere.

The lander rocket motors excavated ~10-20 cm pits that expose possible layering [5, 15, 16] and whose excavation resulted in ejection of numerous relatively reddish clods [5]. There are more pebbles and cobbles (>2 cm) on and/or partially embedded on the west/northwest part of the hollow (Rocky Field) [3-5] where there are ~3x more fragments per m^2 (Fig. 2).

Fragment sphericity, or how equant fragments are, can be defined by the square root of the short axis divided by the long axis as measured in 2D [17-18]. For clasts > ~1 cm and within ~1 m of the lander, sphericity averages 0.84 (range 0.64-1.0, +/- 0.1). By contrast, average sphericity at the Pathfinder, Gusev, and Gale landing sites is 0.72-0.75 (with a broader range, but similar standard deviation) [18-20] and is less in most terrestrial environments [19].

Examination of 872 rocks in and around the hollow reveals various concentrations of mostly buried, embedded, and perched rocks (Fig. 2). Perched rocks represent ~70% those seen on the rim. By contrast, embedded and buried rocks comprise 60% of rocks mapped inside the hollow. There is a slight increase in perched rocks in the higher overall density of rocks exposed at Rocky Field.

The region surrounding Homestead hollow also shows examples of eolian and impact modification. There are nearby bright areas that may mark additional hollows and there are examples of likely ventifacts (e.g., Turtle rock near the lander). The Corintito and Puddle craters within the hollow are just two of 10 that have excavated and redistributed local materials.

Discussion: The attributes of Homestead hollow enable the degradation history to be established [5]. Impact formation, as seems likely [2-5], fragmented the surface and ejected debris resulting in an initial landform whose surface was out of equilibrium with local geomorphic thresholds [5]. Early eolian stripping of the rim and associated partial infilling of the hollow interior likely dominated, leading to more perched rocks on the rim relative to embedded/buried rocks in the interior.

Pristine craters possess relatively steep walls, thereby leading to gravity-driven infilling along the wall whose relative importance also decreased with time as slopes are reduced and the crater is infilled. There is no systematic decrease in the relief of embedded rocks or transition to buried rocks away from the hollow margin, suggesting the initial depth of the depression and subsequent infilling exceeds the scale of observed rocks.

Ongoing impacts continue to play a triple role in hollow degradation: 1) direct modification during formation (e.g., Corintito and The Puddle); 2) short pulses of infilling occurring during emplacement of ejecta from nearby impacts; and 3) generation of fines for additional redistribution/longer pulses of infilling due to the wind. It remains uncertain whether the Rocky Field marks a local ejecta deposit, as there is no obvious source crater. The relatively significant, early eolian rim stripping and concurrent infilling is incomplete (prevailing winds will move some sediment away from the crater), but continues at a greatly diminished rate over time, punctuated by infilling following nearby upwind impacts. Otherwise, sediment production and infilling is limited by very slow weathering and breakdown of resistant basaltic rim blocks, eventually creating a margin characterized mostly by abundant perched rocks.

The partial burial/embedded appearance of many fragments in the hollow and stratigraphy exposed under the lander reflects ongoing, slow infilling of the remaining 0.8 m depression associated with the hollow. Infilling contributions from slow weathering and transport of material from along the hollow rim is likely augmented by dust and occasional influx of eolian sediments during initial degradation of nearby, later forming craters. The apparent competence of the near-surface material implies weak induration [3, 15, 16], perhaps forming a duricrust related to diffusional exchanges of water vapor between the atmosphere and soils [3, 4] as has been observed elsewhere, albeit in lesser thickness [e.g., 21]. Excavation of the pits by the rocket motors produced the numerous, roughly equant, reddish clods that probably contribute to the high sphericity and fragment density in the western workspace.

Comparison to Degradation in Gusev crater: The juxtaposition of attributes of Homestead hollow are comparable to those observed around small craters formed into basaltic rubble in Gusev crater as is their inferred degradation sequence [3, 5, 22-24]. There, early eolian rim stripping and infilling along with gravity-driven slope processes contributed to infilling and rim modification [7, 8] that slowed over time. The result is a 2x-10x concentration of perched rocks along crater rims and more buried rocks inside the Gusev craters [22-24]. Like at Homestead hollow, later rim degradation becomes weathering-limited, punctuated by impacts, and associated infrequent production/transport of fines, and direct emplacement of ejecta.

References: [1] Parker et al. (2019), 50th *LPSC*, 1948. [2] Golombek et al. (2019), 50th *LPSC*, 1694. [3] Golombek et al. (2019), *9th Mars*, this meeting. [4] Warner et al. (2019) 50th *LPSC*, 1184. [5] Grant et al. (2019) 50th *LPSC*, 1199 [6] Fergason, R., et al., (2017), *SSR*, 211, 109-133. [7] Sweeney, J., et al., (2018), *JGR*, 123, 2732-2759. [8] Wilson, S. A. et al. (2019), 50th *LPSC*, 2161. [9] Golombek, M., et al., (2017), *SSR*, 211, 5-95. [10] Warner, N.H., et al., (2017), *SSR*, 211, 147-190. [11] Golombek, M., et al., (2018), *SSR*, 214, 84. [12] Tanaka, K., et al., (2014), *U.S. Geol. Surv. Sci. Invest. Map*, 3292. [13] Calef et al. (2019), 50th *LPSC*, 1977. [14] Weitz et al. (2019), 50th *LPSC*, 1394. [15] Ansan et al. (2019) 50th *LPSC*, 1310. [16] Ansan et al. (2019), *9th Mars*, this meeting. [17] Riley, N.A. (1941), *J. Sed. Petrol*, 11, 94–97. [18] Yingst et al. (2016), *Icarus*, 280, 72-92. [19] Yingst et al. (2007), *JGR*, 112, 0.1029/2005JE002582. [20] Yingst et al. (2008), *JGR*, 113, 10.1029/2008JE003179. [21] Arvidson et al. (2010), *JGR*, 115, 10.1029/2010JE003633. [22] Grant et al. (2004), *Science*, 305, 807-810, 10.1126/science.1099849. [23] Grant et al. (2006), *GRL*, 33, 10.1029/2006GL026964. [24] Grant et al. (2006), *JGR*, 111, 10.1029/2005JE002465.

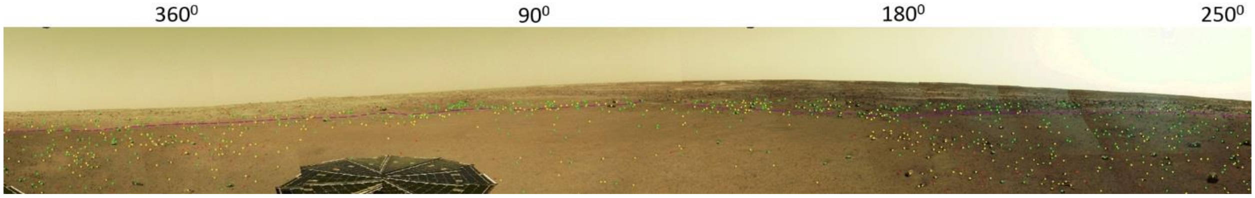

Figure 2. (a) Mosaic covering approximately 290 degrees around the lander with the dashed magenta line denoting the approximate margin of the hollow. Colored dots denoting the relative distribution of buried (red), embedded (yellow), and perched (green) rocks. It is hard to resolve small rocks at distance, the view favors detection of small rocks in hollow, and perched and buried rocks at distance can be blocked by other rocks. Moreover, the viewing angle may preclude detection of some buried rocks near and beyond the edge of the hollow. Nevertheless, the relative abundance of perched rocks along and beyond the hollow rim and of buried and embedded rocks inside the hollow is probably real. IDC Mosaic D_LRGB_0014_RAS030100CYL_R__SCIPANQM1.